Science Advances
AAAS

Supplementary Materials for

Activation of CGRP receptor–mediated signaling promotes tendon-bone healing

Xibang Zhao *et al.*

Corresponding author: Jiali Wang, wangjli8@mail.sysu.edu.cn

Sci. Adv. **10**, eadg7380 (2024)
DOI: 10.1126/sciadv.adg7380

This PDF file includes:

Supplementary Figure and Table Legends

Fig. S1 Adenovirus vector profile and sequence. (**A**) Scramble adenovirus. (**B**) Adenovirus sh*Calcrl* #1. (**C**) Adenovirus sh*Calcrl* #2. (**D**) Adenovirus sh*Calcrl* #3. (**E**) Adenovirus Calcrl (NM_018782.2).

Fig. S2 Gene transfection efficiency of BMSCs incubated with different adenoviral plasmids. (A) Adenovirus shCalcrl #1. (**B**) Adenovirus shCalcrl #2. (**C**) Adenovirus shCalcrl #3. (**D**) Adenovirus *Calcrl* (NM_018782.2). Scale bars: 100 μm.

Fig. S3 The schematic diagram showing the surgical and treatment process (A) and the detailed process conducted in mice (B). I: incisions made around the knee joint; II: isolation of tendon graft from gastrocnemius tendon; III: exposure of the knee joint; IV: fixation of two ends of the tendon graft with sutures; V: transection of ACL; VI: creation of bone tunnel and injection of HMPs; VII: placement of the tendon graft and fixation at the femoral exit and the tibial entrance; VIII: closure of the wound. **(C) The animal number assigned for each testing in each group at different time points.**

Fig. S4 The effect of CGRP on calcium nodule formation in both mouse BMSC (mBMSC) (A) and human BMSC (hBMSC) (B) at 14 days and 21 days after osteogenic differentiation through quantitative analysis of Alizarin Red stained minerals.*P<0.05, **P<0.01 and ***P<0.001, n=3 independent biological replicates. The Blank indicates BMSCs without incubation in osteogenic induction medium (OIM).

Fig. S5 The effect of CGRP on osteogenic differentiation capability of rat BMSCs and MC3T3-E1. (A) Gene expression levels of *Sp7*, *Runx2*, osteocalcin (*Ocn*), and osteopontin (*Opn*) of rat derived BMSCs after incubation in OIM with or without CGRP. *P<0.05, **P<0.01, n=3 individual biological replicates. (B) Gene expression levels of *Sp7*, *Runx2*, *Ocn*, and *Opn* of MC3T3-E1 after incubation in OIM with or without CGRP. ns: not significant, *P<0.05, **P<0.01, ***P<0.001, n=3 individual biological replicates. (C) WB analysis of protein levels of OSX, p-CREB, CREB, PKA, and GAPDH in MC3T3-E1 after incubation in OIM with or without CGRP. The Blank indicates BMSCs without incubation in osteogenic induction medium (OIM).

Fig. S6 The effect of CGRP on osteogenic differentiation capability of human BMSCs. (**A**) Real-time PCR analysis of *Sp7*, *Runx2*, osteocalcin (*Ocn*), osteopontin (*Opn*) and *Calcrl* mRNA expression in the BMSCs after treatment with CGRP. *P<0.05, **P<0.01 and ***P<0.001, n=3 independent biological replicates. (**B**) WB analysis of

protein levels of RUNX2, OSX, p-CREB, CREB, CALCRL and GAPDH in BMSCs with or without treatment of CGRP. (**C**) Quantification of RUNX2/GAPDH ratio, OSX/GAPDH ratio, and p-CREB/CREB ratio, and CALCRL/GAPDH ratio by WB analysis from (**B**). (**D**) WB analysis of protein levels of OSX, JUNB, SHH, p-CREB, CREB, and GAPDH in BMSCs with or without treatment of CGRP or H-89, a selective inhibitor of cyclic AMP-dependent protein kinase (PKA). *P<0.05, **P<0.01 and ***P<0.001, n=3 independent biological replicates. (**E**) Quantification of OSX/GAPDH ratio, JUNB/GAPDH, p-CREB/CREB ratio, and SHH/GAPDH ratio by WB analysis from (**D**). The Blank indicates BMSCs without incubation in osteogenic induction medium (OIM).

Fig. S7 Representative immunofluorescence staining of JUNB and NF200 at the tendon-bone interface in mice and the quantitative analysis of relative intensity of JUNB$^+$ area at 4 weeks and 6 weeks post-surgery. Dotted line: tendon graft boundary; B: bone; T: tendon; IF: interface. Scale bar: 200 μm. *P<0.05, **P<0.01, and ***P<0.001, n=3.

Fig. S8 The fluorescence intensity of CGRP$^+$, NF200$^+$, CGRP$^+$NF200$^+$, and SHH$^+$ area at the tendon-bone interface in mice. (A) Representative immunofluorescence staining of CGRP, NF200, and their co-immunostaining at the tendon-bone interface in mice at 4 weeks and 6 weeks post-surgery. Dotted line: tendon graft boundary; B: bone; T: tendon; IF: interface. Scale bar: 200 μm. (B) Representative immunofluorescence staining of SHH at the tendon-bone interface in mice at 4 weeks and 6 weeks post-surgery. Dotted line: tendon graft boundary; B: bone; T: tendon; IF: interface. Scale bar: 200 μm. (C) Quantitative analysis of relative fluorescence intensity of CGRP$^+$NF200$^+$ and SHH$^+$ area at the tendon-bone interface in mice at 4 weeks and 6 weeks post-surgery. *P<0.05, **P<0.01, ***P<0.001, and ****P<0.0001, n=3.

Fig. S9 The expression level changes of CGRP and CALCRL at the trabecular bone in mice from pre-surgery to post-surgery. *P < 0.05, n=3. Dotted line: tendon graft boundary; B: bone; T: tendon; IF: interface.

Fig. S10 Real-time whole-body imaging of mice at different time points after intra-articular injection of the fluorescent dye Cy5 grafted HMPs (HMP@Cy5) and PBS by In Vivo Imaging System (IVIS). The HMPs continued to degrade in the knee joint cavity after injection and a complete degradation was observed after 24 days within a 30-day experimental period.

Fig. S11 The fluorescence intensities of $CD31^+$, $NF200^+$ and $RUNX2^+$ area as well as the ratios of CALCRL overlapping CD31, NF200, or RUNX2 at the tendon-bone interface in mice with or without adv-*Calcrl* treatment. (A) Representative immunofluorescence staining of CD31, NF200, RUNX2, and their co-immunostaining with CALCRL at the tendon-bone interface in mice without or with adv-*Calcrl* treatment at 1 week, 2 weeks, 4 weeks, and 6 weeks post-surgery. Dotted line: tendon graft boundary; B: bone; T: tendon; IF: interface. Scale bar: 200 μm. (B) Quantitative analysis of relative fluorescence intensities of $CD31^+$, $NF200^+$, and $RUNX2^+$ area at the tendon-bone interface in the control group and the adv-*Calcrl* group at 1 week, 2 weeks, 4 weeks, and 6 weeks post-surgery. *P<0.05, **P<0.01, ***P<0.001, n=3. (C) The ratios of CALCRL overlapping CD31, NF200, or RUNX2 at the tendon-bone interface in the control group and the adv-*Calcrl* group at 1 week, 2 weeks, 4 weeks, and 6 weeks post-surgery. ns: not significant, *P<0.05, **P<0.01, ***P<0.001, and ****P<0.0001, n=3.

Fig. S12 Schematic illustration of healing mechanism at the tendon-bone interface modulated by CGRP receptor-mediated signaling in mice after adenoviral transfection through HMP controlled release. The activation of CGRP receptor-mediated signaling promotes the production of osteoblasts, which may be a driving force facilitating innervation and type H vessel formation at the TBI through upregulation of SHH and SLIT3, respectively.

Fig. S13 Representative histologic images showing the tendon-bone interface in both the control group and the adv-*Calcrl* group at 6 weeks and 8 weeks post-surgery by Hematoxylin &Eosin (H&E) staining (left) and healing quality assessment using histologic scores. ns: not significant, n=5.

Fig. S14 The effect of SLIT3 treatment on graft healing. (A) Representative immunofluorescence staining of NF200 and CD31 and quantitative analysis of their relative fluorescence intensities at the tendon-bone interface in mice with various treatments at 2 weeks post-surgery. Dotted line: tendon graft boundary; B: bone; T: tendon; IF: interface. Scale bar: 200 μm. (B) Quantitative analysis of gait performance and load to failure in mice with various treatments at 6 weeks post-surgery. ns: not significant, *P < 0.05, **P < 0.01, ***P < 0.001, and ****P<0.0001, n=3.

Fig. S15 The adv-*Calcrl* and adv-sh*Calcrl* injection show no health risks within a short-term period. (A) Hematological characteristics of mice after treatment for 2 days

and 4 days, respectively. The treatment indicates injection of HMPs loading PBS, scramble shRNA, adv-*Calcrl*, or adv-sh*Calcrl*. The reference range was indicated by the dotted line. n=3. (B) Representative immunofluorescence staining of F4/80 assigned for macrophage at the tendon-bone interface in mice with different treatments at 2 weeks post-surgery. Dotted line: tendon graft boundary; B: bone; T: tendon; IF: interface.

Table S1 Primer sequences used for real-time quantitative reverse transcriptase polymerase chain reaction (qRT-PCR)

Table S2 Histologic Scoring Criteria for semi-quantitative analysis of the tendon-bone interface healing.

Fig. S1

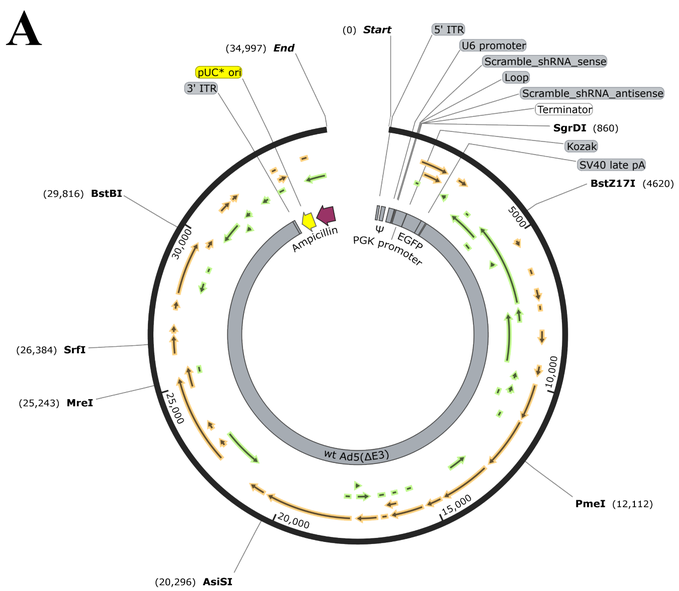

Mammalian knockdown vector; Adenovirus shRNA knockdown vector Scramble.
34,997 bp

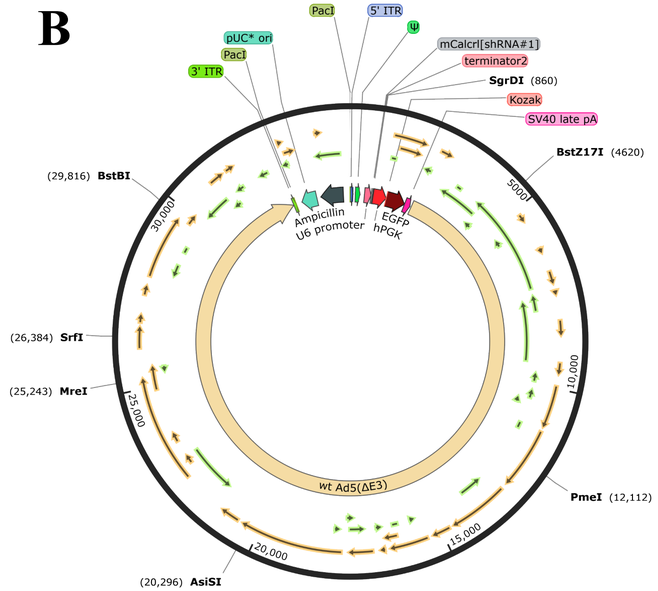

Mammalian knockdown vector; Adenovirus shRNA knockdown vector#1.
34,997 bp

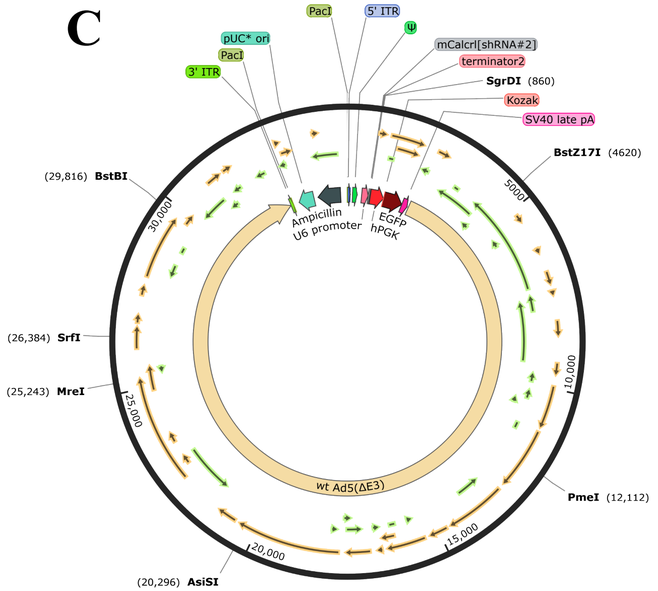

Mammalian knockdown vector; Adenovirus shRNA knockdown vector#2.
34,997 bp

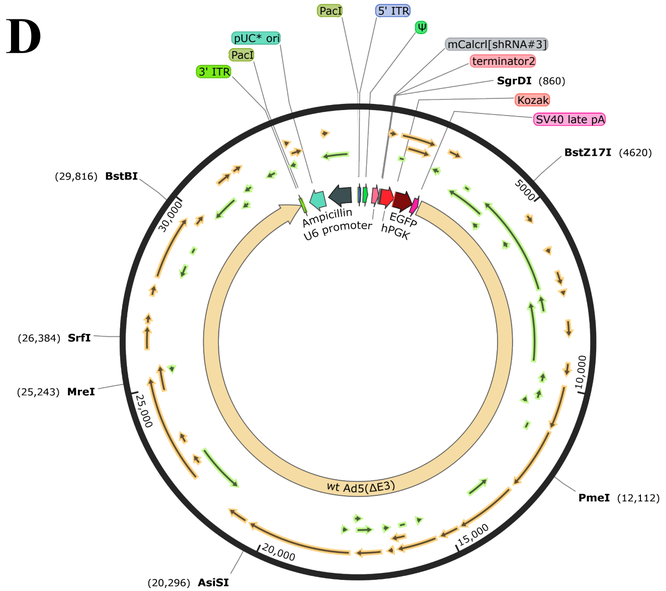

Mammalian knockdown vector; Adenovirus shRNA knockdown vector#3.
34,997 bp

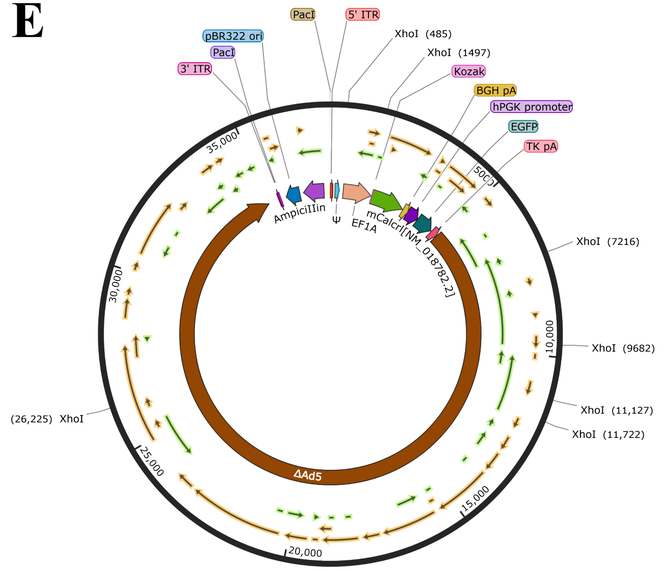

Mammalian overexpression vector; Adenovirus mCalcrl[NM_018782.2] vector.
37,570 bp

Fig. S2

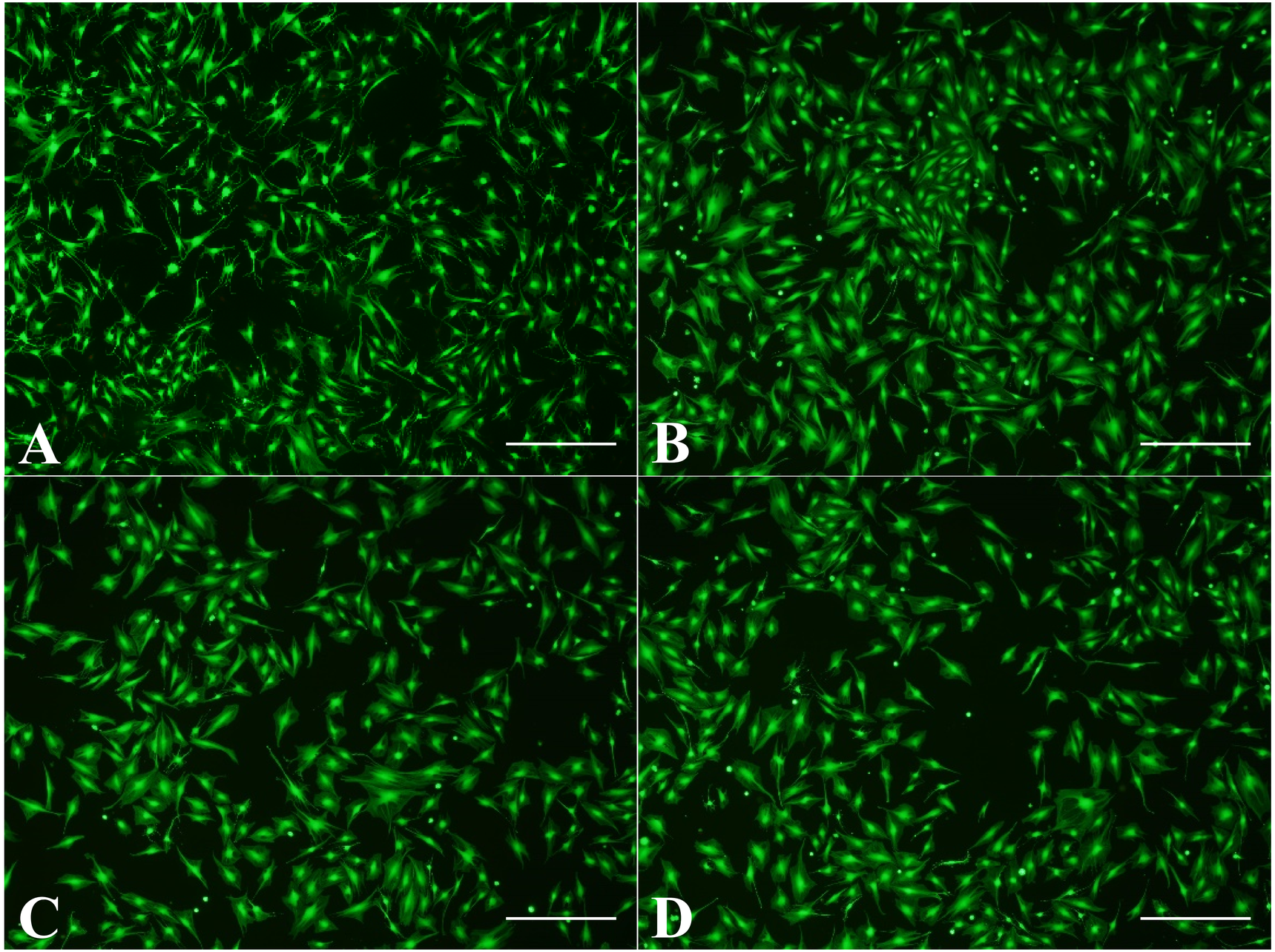

Fig. S3

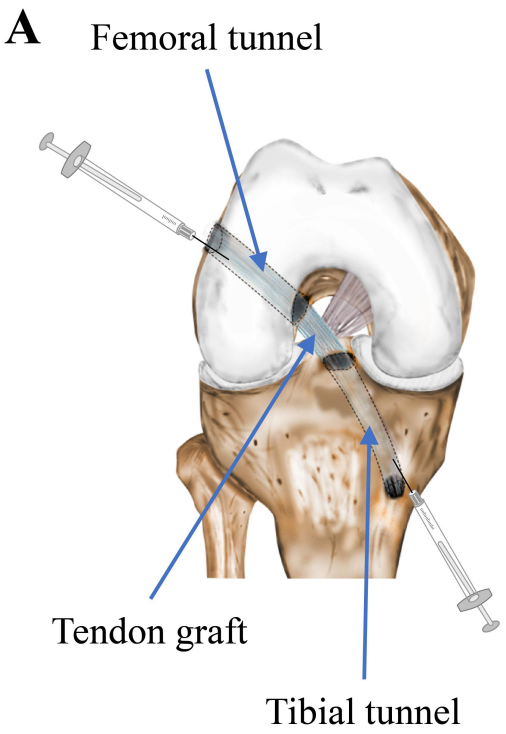

C

Mice with ACL reconstruction

Healthy
Sham
Control
Adv-sh*Calcrl*
Adv-*Calcrl*

0 day *1 w* *2 w* *4 w* *6 w*

						Subtotal
Gait analysis	●●●●●	5	5	5	5	25
Histology	●●●	5	5	5	5	60
Micro-CT	●●●					
Mechanical Testing	●●●			5	5	30
	●			3	3	6
					Total	121

Note: n=5 for H&E and Safranin&O staining, n=4-5 for micro-CT analysis while n=3 for immunofluorescence staining.

Fig. S4

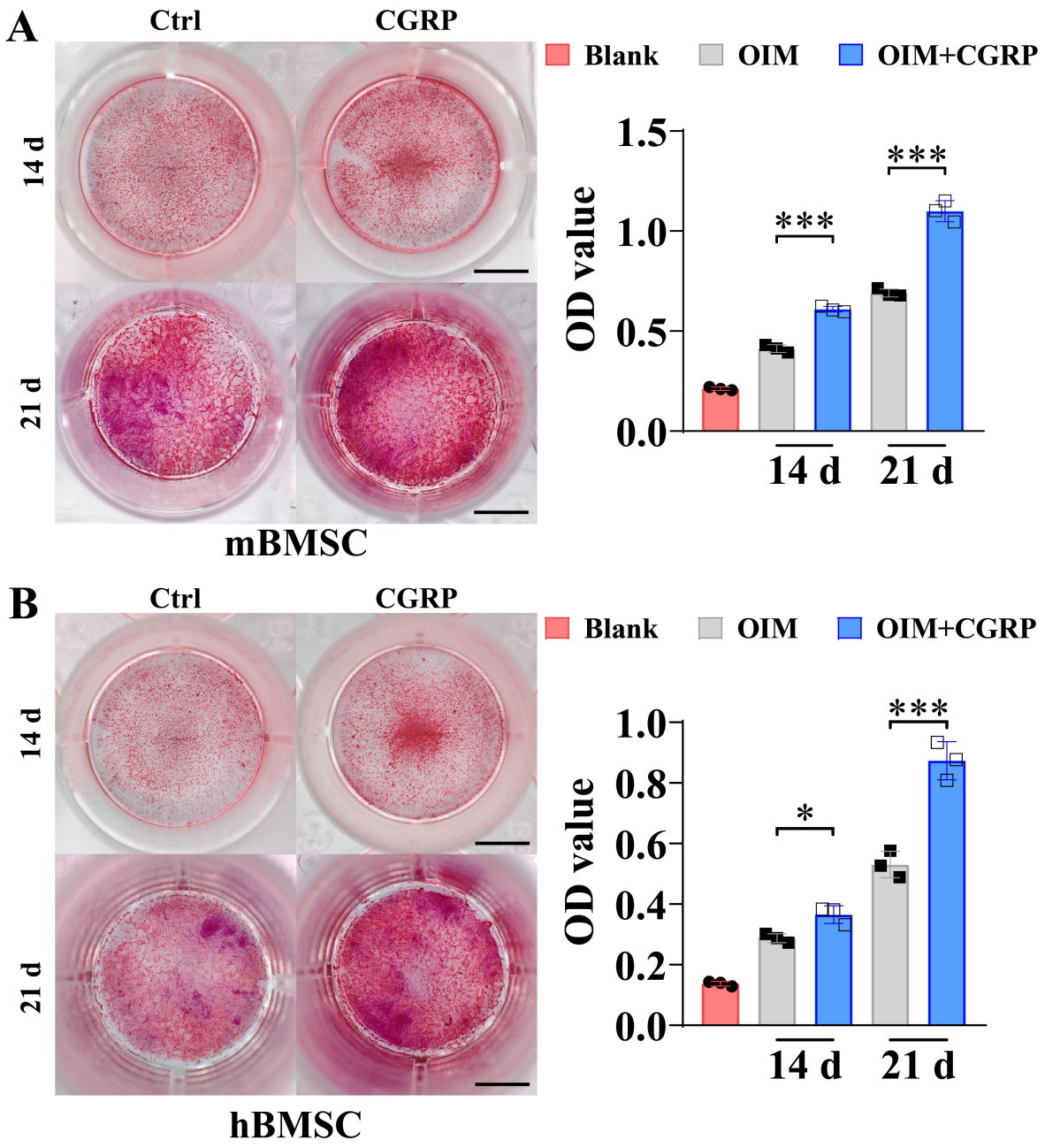
A
Ctrl
CGRP
14 d
21 d
mBMSC
Blank
OIM
OIM+CGRP
OD value
1.5
1.0
0.5
0.0
***
***
14 d
21 d
B
Ctrl
CGRP
14 d
21 d
hBMSC
Blank
OIM
OIM+CGRP
OD value
1.0
0.8
0.6
0.4
0.2
0.0
*
***
14 d
21 d

Fig. S5

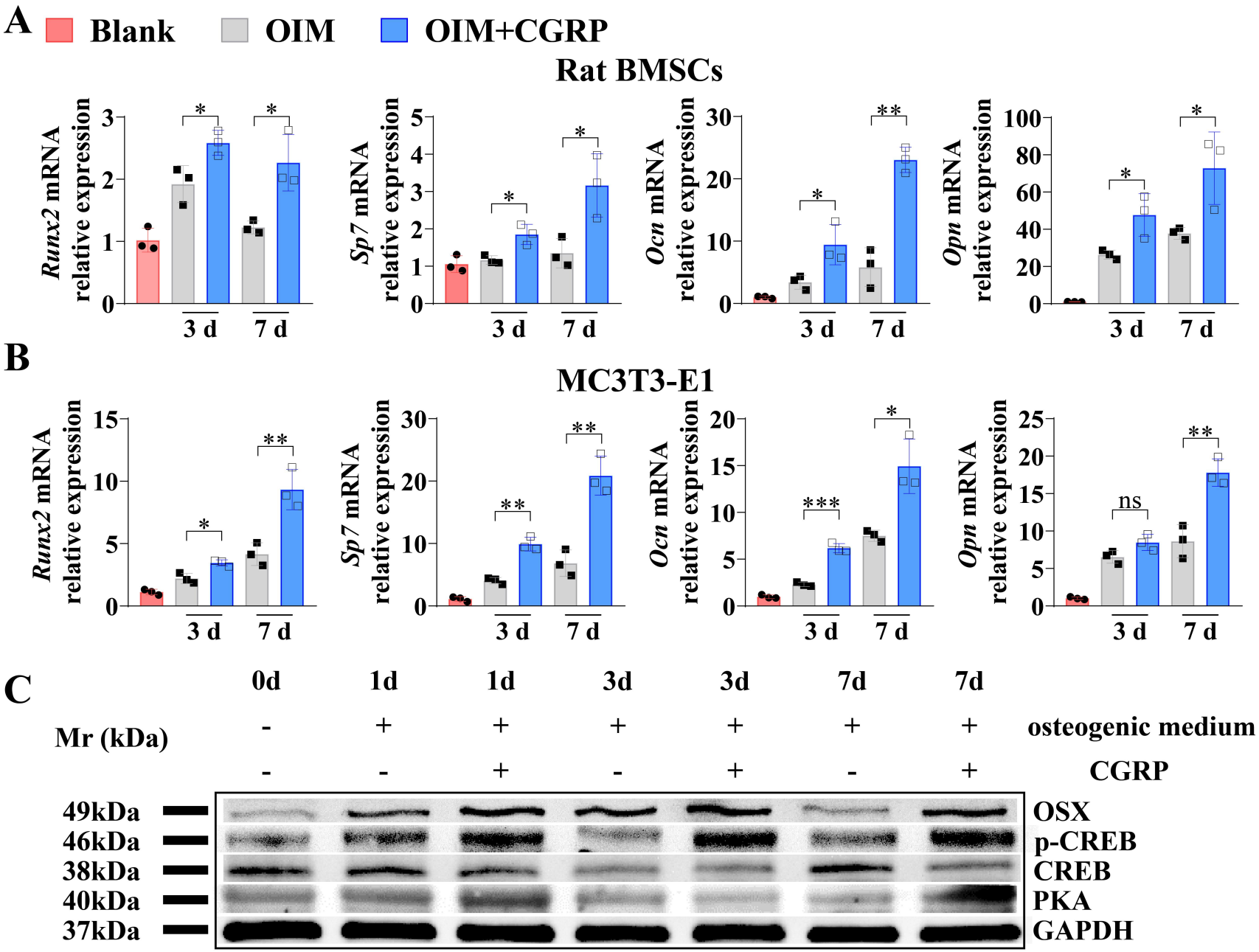
A
Blank
OIM
OIM+CGRP
Rat BMSCs
Runx2 mRNA relative expression
Sp7 mRNA relative expression
Ocn mRNA relative expression
Opn mRNA relative expression
3 d
7 d
B
MC3T3-E1
Runx2 mRNA relative expression
Sp7 mRNA relative expression
Ocn mRNA relative expression
Opn mRNA relative expression
ns
C
0d
1d
1d
3d
3d
7d
7d
Mr (kDa)
osteogenic medium
CGRP
49kDa
46kDa
38kDa
40kDa
37kDa
OSX
p-CREB
CREB
PKA
GAPDH

Fig. S6

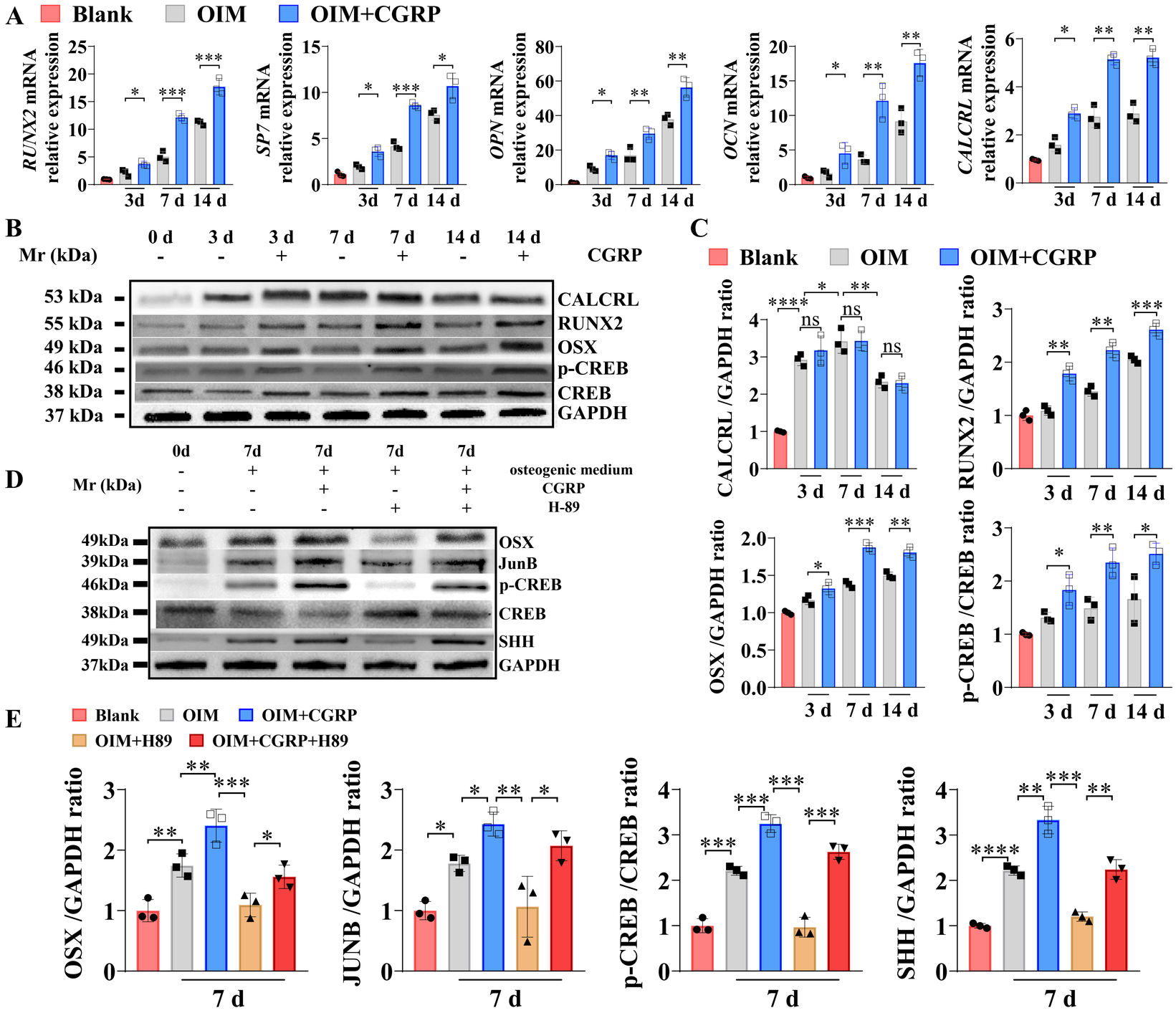
A
Blank
OIM
OIM+CGRP
RUNX2 mRNA relative expression
SP7 mRNA relative expression
OPN mRNA relative expression
OCN mRNA relative expression
CALCRL mRNA relative expression
3d
7 d
14 d
B
Mr (kDa)
0 d
3 d
3 d
7 d
7 d
14 d
14 d
CGRP
53 kDa
55 kDa
49 kDa
46 kDa
38 kDa
37 kDa
CALCRL
RUNX2
OSX
p-CREB
CREB
GAPDH
C
Blank
OIM
OIM+CGRP
CALCRL /GAPDH ratio
RUNX2 /GAPDH ratio
OSX /GAPDH ratio
p-CREB /CREB ratio
ns
3 d
7 d
14 d
D
Mr (kDa)
0d
7d
7d
7d
7d
osteogenic medium
CGRP
H-89
49kDa
39kDa
46kDa
38kDa
49kDa
37kDa
OSX
JunB
p-CREB
CREB
SHH
GAPDH
E
Blank
OIM
OIM+CGRP
OIM+H89
OIM+CGRP+H89
OSX /GAPDH ratio
JUNB /GAPDH ratio
p-CREB /CREB ratio
SHH /GAPDH ratio
7 d

Fig. S7

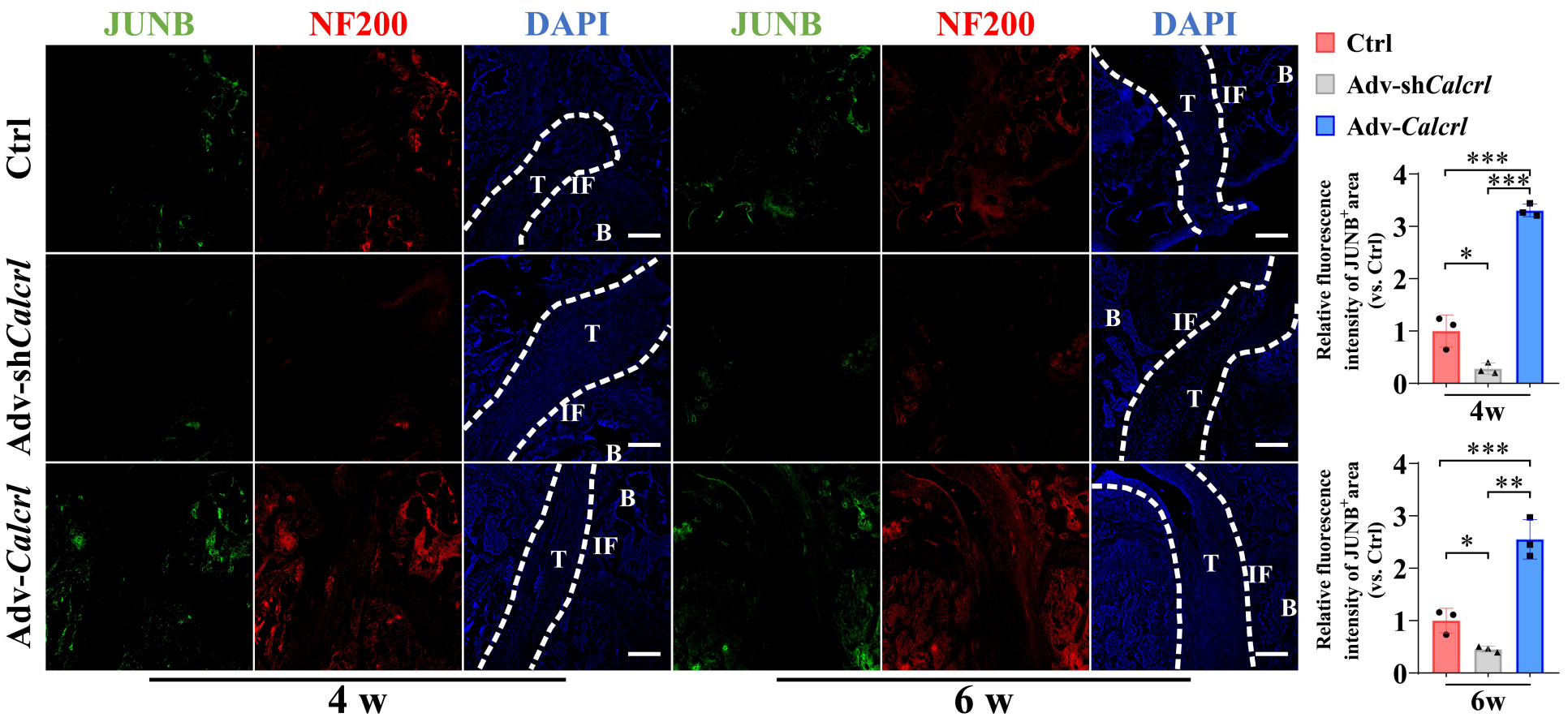
JUNB
NF200
DAPI
JUNB
NF200
DAPI
Ctrl
Adv-shCalcrl
Adv-Calcrl
T
IF
B
4 w
6 w
Ctrl
Adv-shCalcrl
Adv-Calcrl
Relative fluorescence intensity of JUNB+area (vs. Ctrl)
4w
6w
***
**
*

Fig. S8

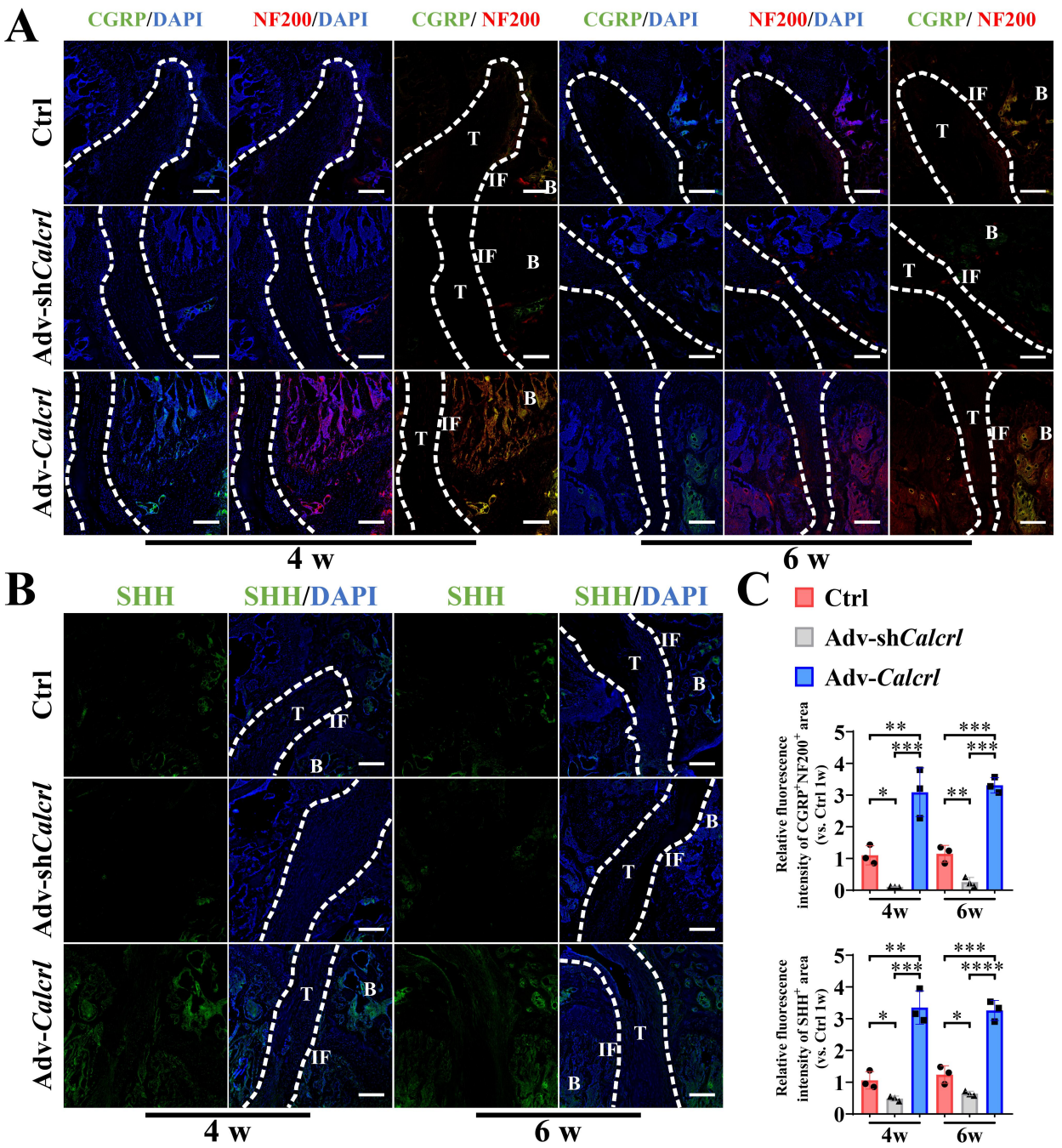
A
CGRP/DAPI
NF200/DAPI
CGRP/ NF200
CGRP/DAPI
NF200/DAPI
CGRP/ NF200
Ctrl
Adv-shCalcrl
Adv-Calcrl
T
IF
B
4 w
6 w
B
SHH
SHH/DAPI
SHH
SHH/DAPI
Ctrl
Adv-shCalcrl
Adv-Calcrl
T
IF
B
4 w
6 w
C
Ctrl
Adv-shCalcrl
Adv-Calcrl
Relative fluorescence intensity of CGRP+NF200+ area (vs. Ctrl 1w)
Relative fluorescence intensity of SHH+ area (vs. Ctrl 1w)
4w
6w

Fig. S9

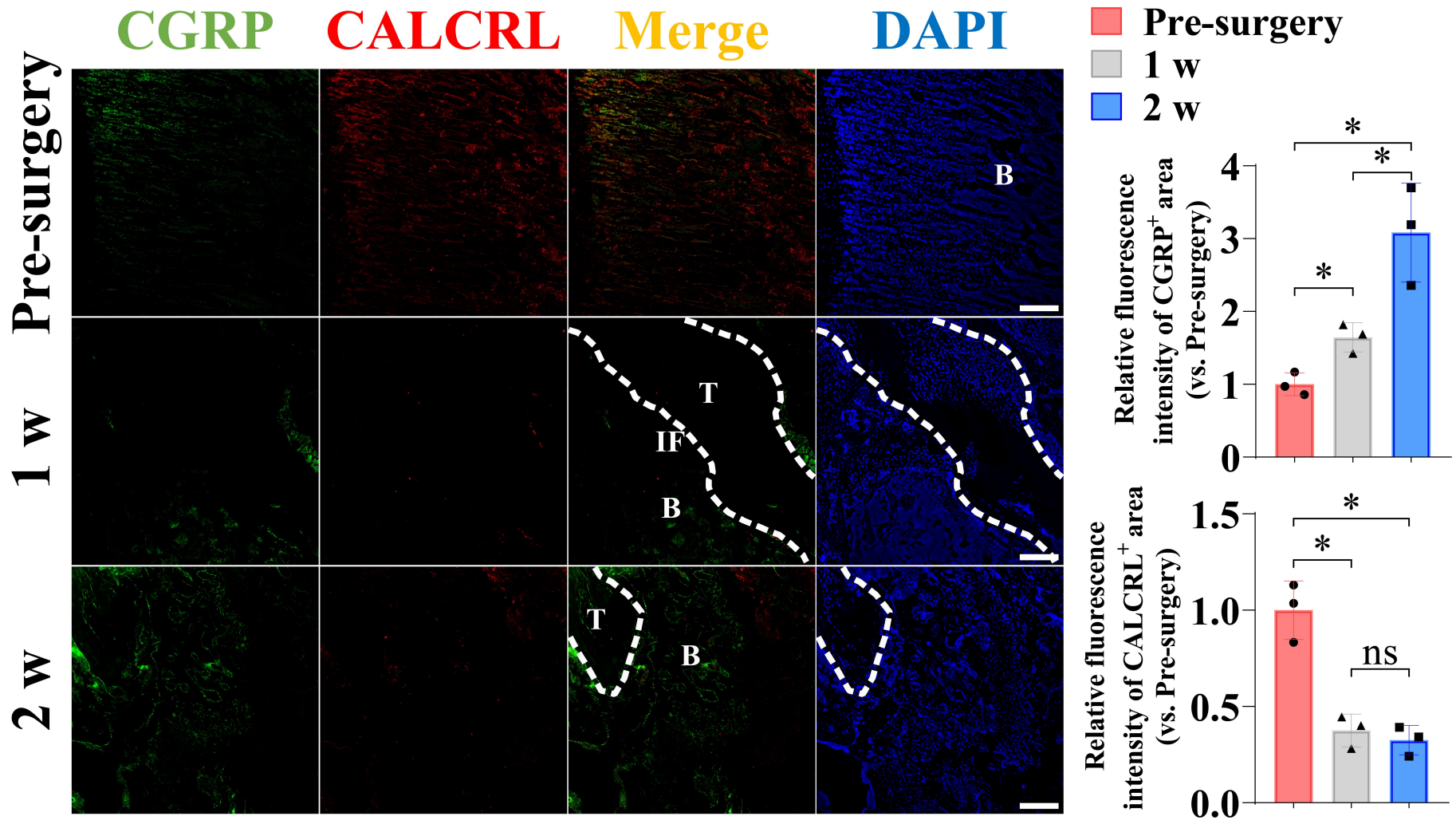
CGRP
CALCRL
Merge
DAPI
Pre-surgery
1 w
2 w
B
T
IF
B
T
B
Pre-surgery
1 w
2 w
Relative fluorescence intensity of CGRP+ area (vs. Pre-surgery)
0
1
2
3
4
*
*
*
Relative fluorescence intensity of CALCRL+ area (vs. Pre-surgery)
0.0
0.5
1.0
1.5
*
*
ns

Fig. S10

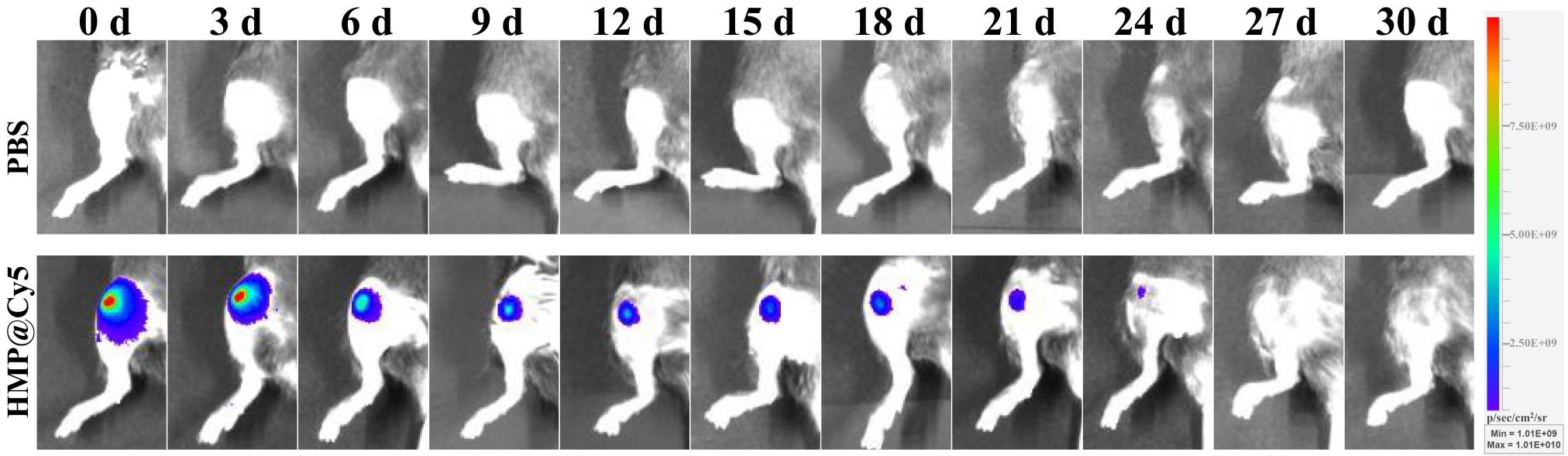
0 d
3 d
6 d
9 d
12 d
15 d
18 d
21 d
24 d
27 d
30 d
PBS
HMP@Cy5
7.50E+09
5.00E+09
2.50E+09
p/sec/cm²/sr
Min = 1.01E+09
Max = 1.01E+010

Fig. S11

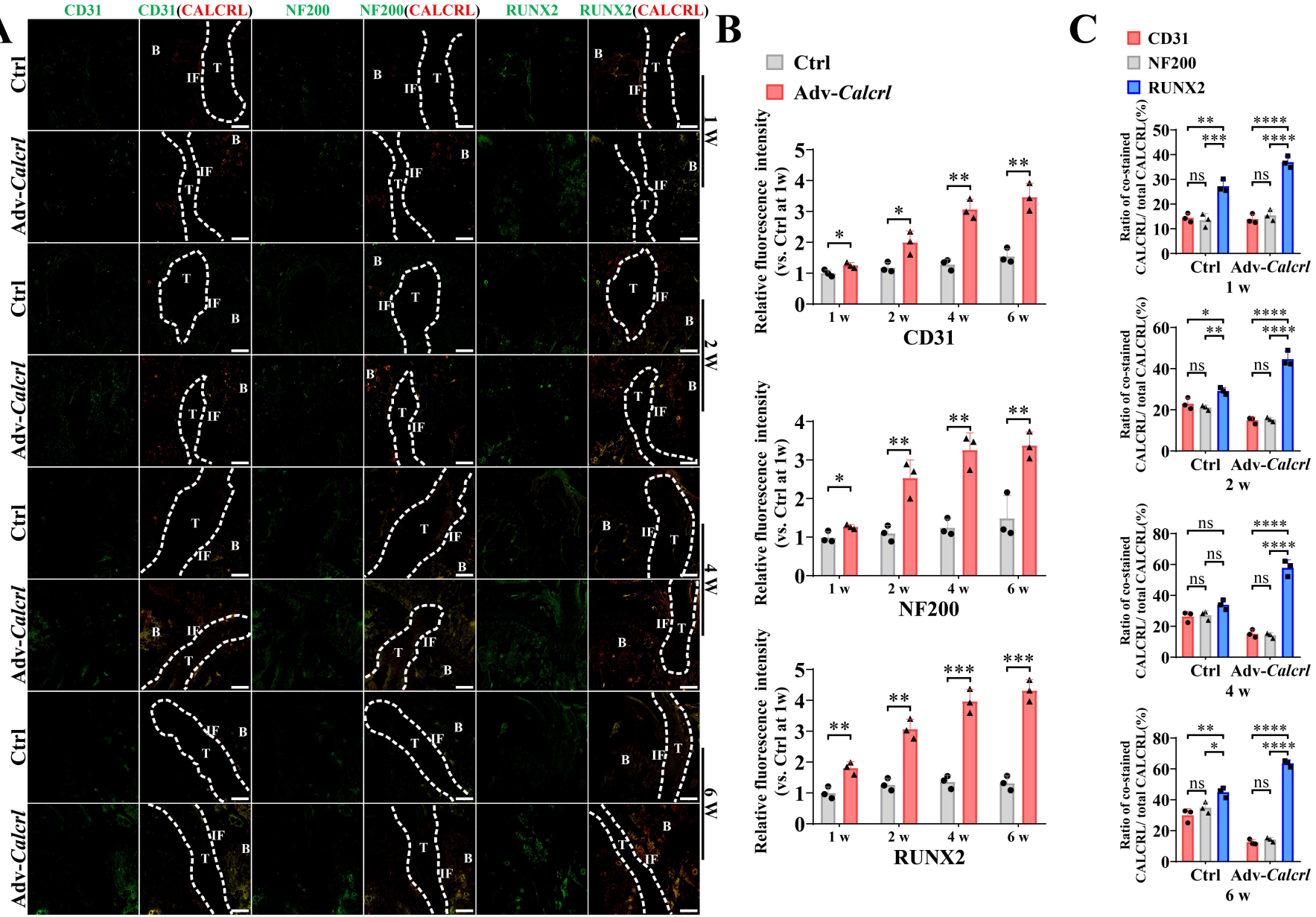
A
CD31
CD31(CALCRL)
NF200
NF200(CALCRL)
RUNX2
RUNX2(CALCRL)
Ctrl
Adv-Calcrl
1W
2 W
4 W
6 W
B
Ctrl
Adv-Calcrl
Relative fluorescence intensity (vs. Ctrl at 1w)
1 w
2 w
4 w
6 w
CD31
NF200
RUNX2
C
CD31
NF200
RUNX2
Ratio of co-stained CALCRL/ total CALCRL(%)
Ctrl
Adv-Calcrl
1 w
2 w
4 w
6 w

Fig. S12

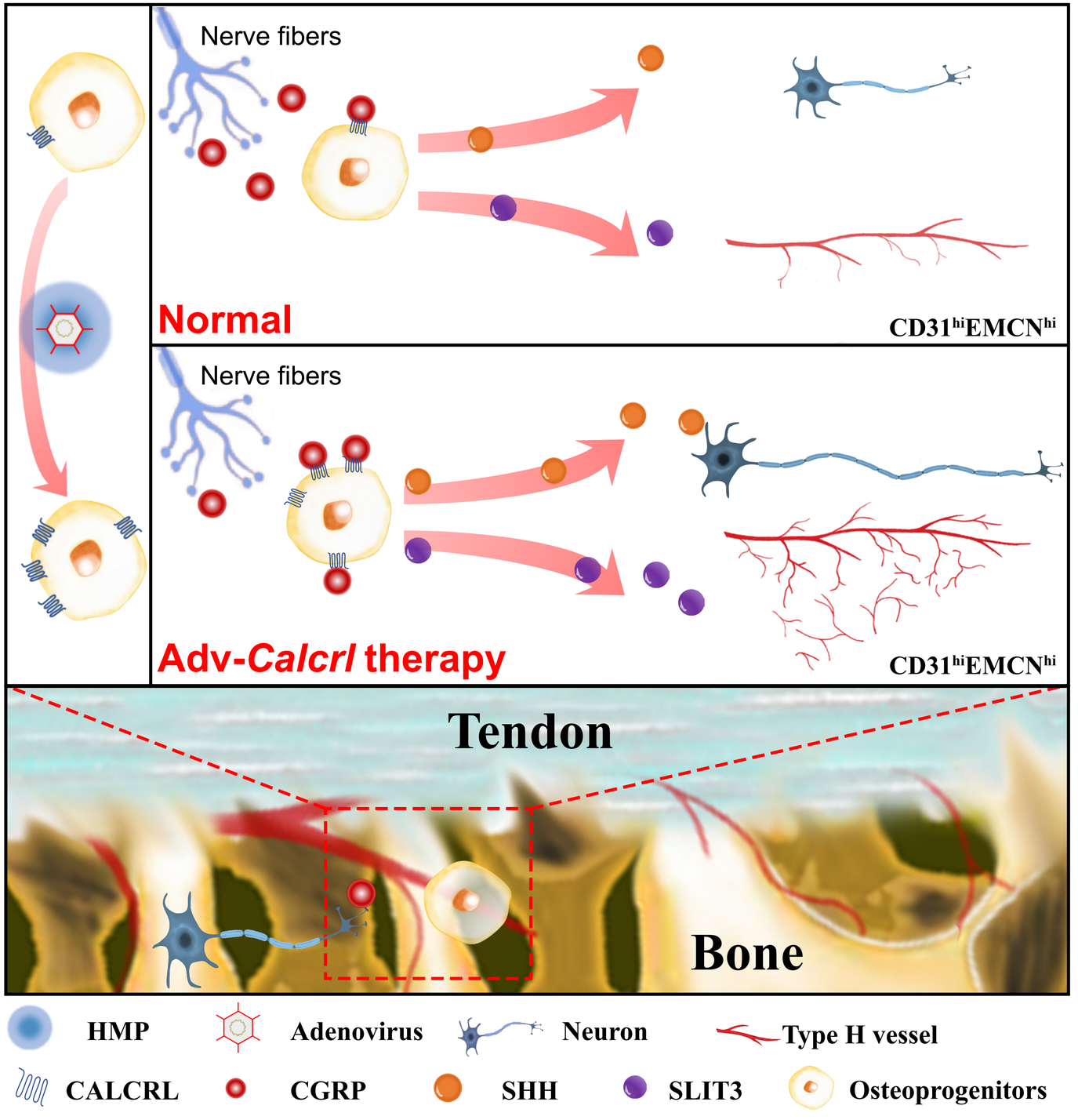
Nerve fibers
Normal
CD31hiEMCNhi
Nerve fibers
Adv-Calcrl therapy
CD31hiEMCNhi
Tendon
Bone
HMP
Adenovirus
Neuron
Type H vessel
CALCRL
CGRP
SHH
SLIT3
Osteoprogenitors

Fig. S13

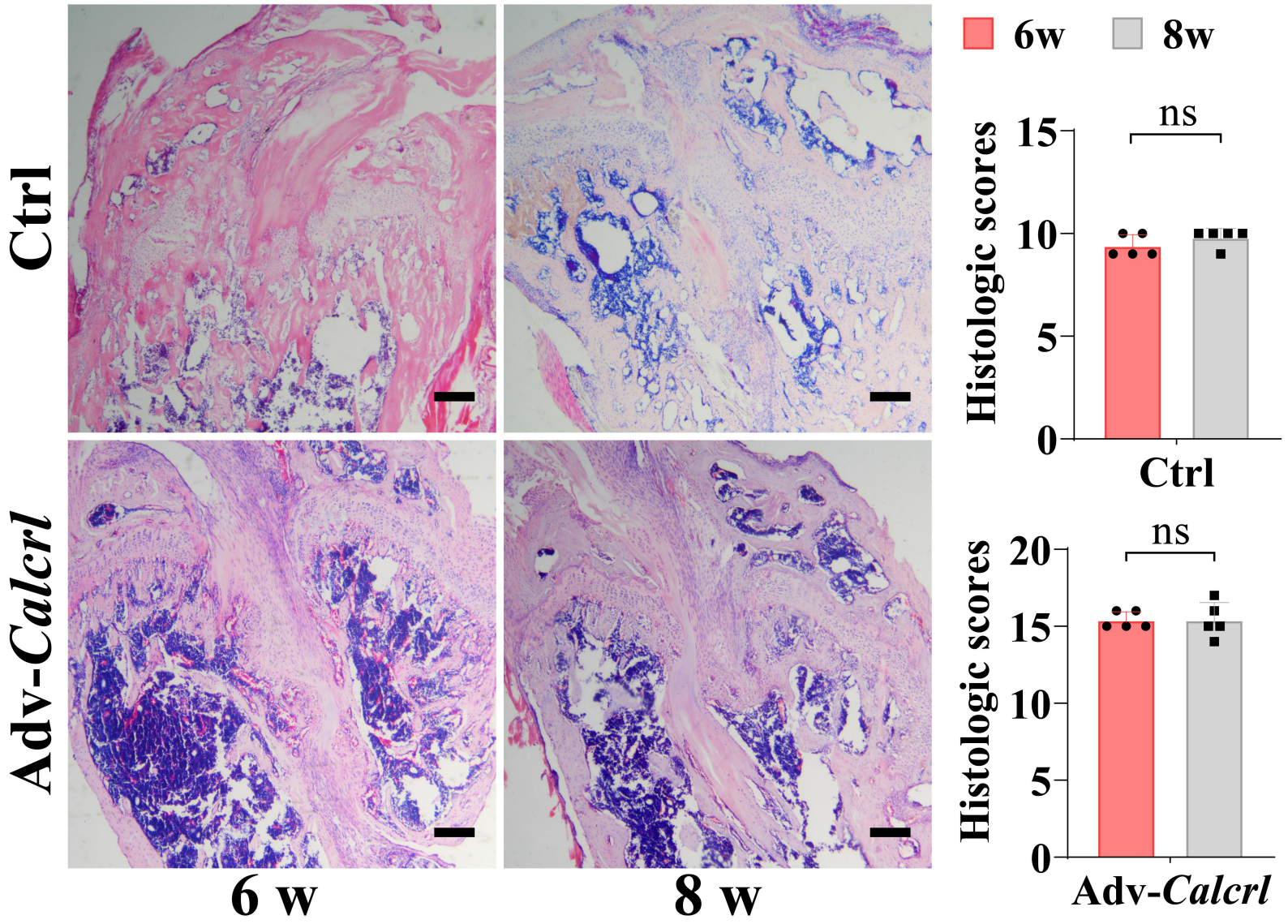
Ctrl
Adv-Calcrl
6 w
8 w
6w
8w
ns
Histologic scores
15
10
5
0
Ctrl
ns
Histologic scores
20
15
10
5
0
Adv-Calcrl

Fig. S14

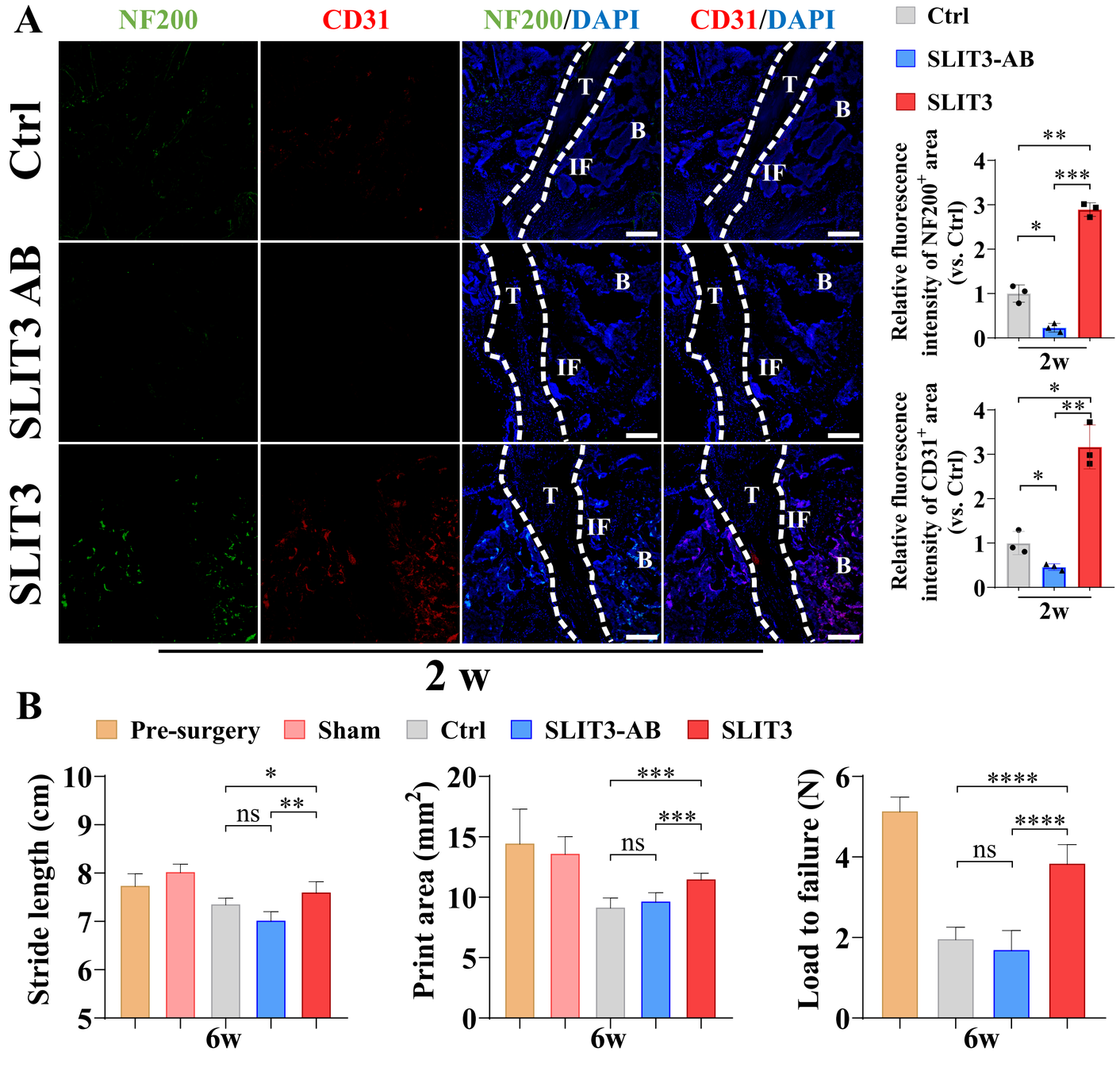
A
NF200
CD31
NF200/DAPI
CD31/DAPI
Ctrl
SLIT3 AB
SLIT3
T
B
IF
2 w
Ctrl
SLIT3-AB
SLIT3
Relative fluorescence intensity of NF200+ area (vs. Ctrl)
Relative fluorescence intensity of CD31+ area (vs. Ctrl)
2w
B
Pre-surgery
Sham
Ctrl
SLIT3-AB
SLIT3
Stride length (cm)
Print area (mm2)
Load to failure (N)
6w
ns

Fig. S15

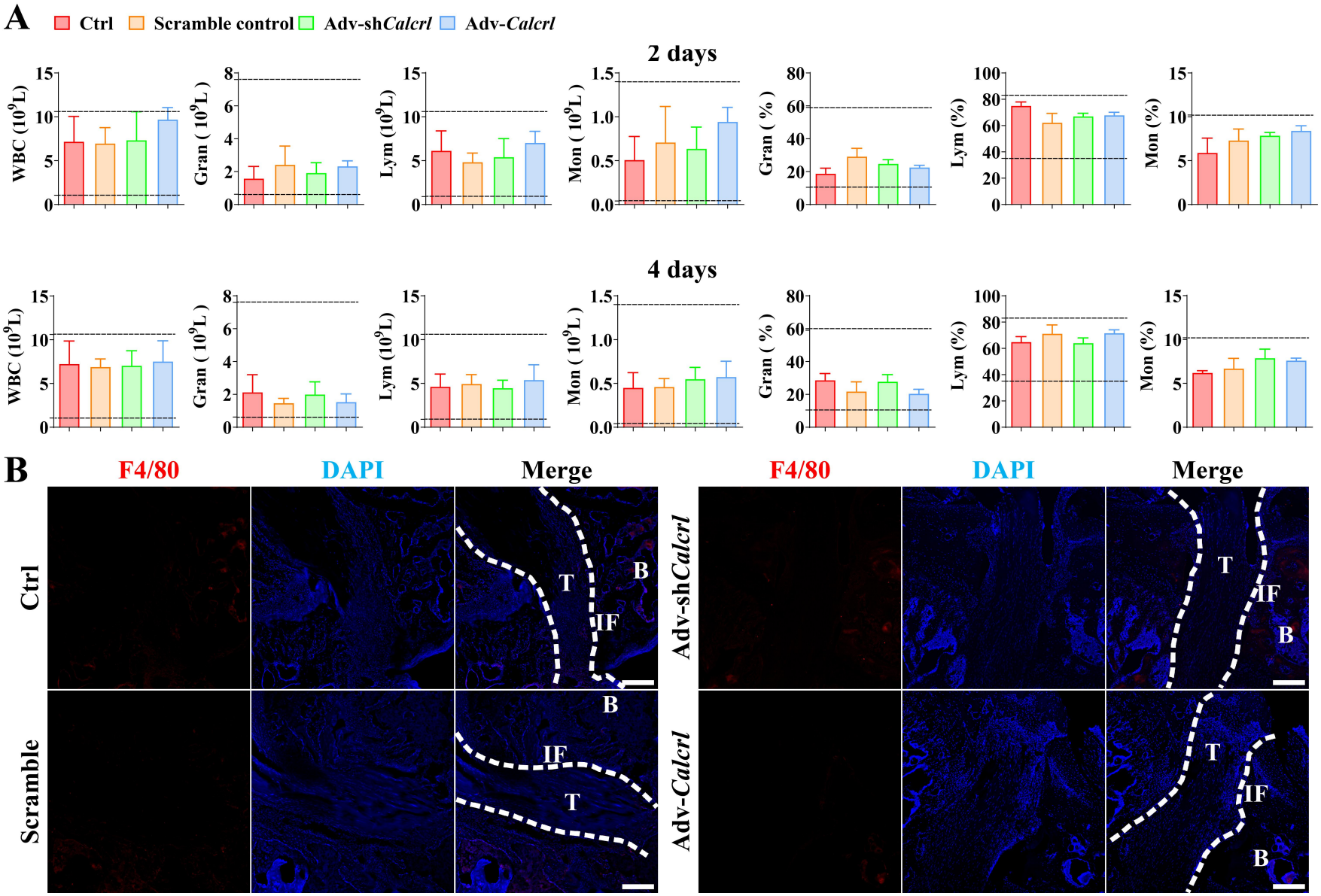
A
Ctrl
Scramble control
Adv-shCalcrl
Adv-Calcrl
2 days
4 days
WBC (10^9L)
Gran (10^9L)
Lym (10^9L)
Mon (10^9L)
Gran (%)
Lym (%)
Mon (%)
B
F4/80
DAPI
Merge
Ctrl
Scramble
Adv-shCalcrl
Adv-Calcrl
T
IF
B

Table S1

Table S1. Primer sequences used for real-time quantitative reverse transcriptase polymerase chain reaction (qRT-PCR)

Gene name (ID)	Forward primer sequence (5'>3')	Reverse primer sequence (5'>3')
Runx2 (ID: 12393)	CTGGCGGTGCAACAAG	CAGCGGAGGCATTTCG
Sp7 (ID: 170574)	CACCAGGTCCAGGCAACA	GAGCAAAGTCAGATGGGTAAGT
Ocn (ID: 12096)	GAGGGCAATAAGGTAGTGAA	CATAGATGCGTTTGTAGGC
Opn (ID: 20750)	ATGAGACCGTCACTGCTA	CTCAGTCCATAAGCCAAG
Gapdh (ID: 14433)	AAATGGTGAAGGTCGGTGTGAAC	AACAATCTCCACTTTGCCACTG
Calcrl (ID: 54598)	AATCATCCACCTCACGG	AAGTAGTTACAGCCCATCA
RUNX2 (ID: 860)	CTACTATGGCACTTCGTCAGG	TCCATCAGCGTCAACACC
SP7 (ID: 121340)	CCTCCTGCGACTGCCCTAA	GCGAAGCCTTGCCATACA
OCN (ID: 632)	GGCAGCGAGGTAGTGAAGA	CCTGAAAGCCGATGTGGT
OPN (ID: 6696)	GTTTCGCAGACCTGACATCC	TTCAACTCCTCGCTTTCCAT
GAPDH (ID: 2597)	CAGGAGGCATTGCTGATGAT	GAAGGCTGGGGCTCATTT
CALCRL (ID: 10203)	ATTGTGGTGGCCGTGTTT	TGGATAATGTAGAGGAGATGGGT
Runx2 (ID: 367218)	CCCAACTTCCTGTGCTCC	AGTGAAACTCTTGCCTCGTC
Sp7 (ID: 300260)	CCCTCTGCGAGACTCAACA	TGCCCACCACCTAACCAA
Ocn (ID: 25295)	GGGCAGTAAGGTGGTGAA	GTCCTGGAAGCCAATGTG
Opn (ID: 25353)	AGGAGTTTCCCTGTTTCTG	GTCTTCCCGTTGCTGTC
Gapdh (ID: 24383)	GACATGCCGCCTGGAGAAAC	AGCCCAGGATGCCCTTTAGT

Table S2

Table S2. Histologic Scoring Criteria for semi-quantitative analysis of the tendon-bone interface healing.

	0	1	2	3	4
Cellularity	Separation	Marked	Moderate	Mild	Minimal
Cellular morphology of interface tissue	Only fibrovascular tissue	Fibrous tissue with Sharpey-like fibers <50%	Fibrous tissue with Sharpey-like fibers ≥50%	Fibrocartilage with mature cartilage cells <50%	Fibrocartilage with mature cartilage cells ≥50%
Extent of fibrocartilage tissue surrounding tendon	Not visible	Slightly surrounded (<25%)	Partially surrounded (25%-50%)	Moderately surrounded (50%-75%)	Mostly surrounded (≥75%)
Interface tissue transition from bone to tendon	Discontinuous	Continuous but slightly indistinct (<25%)	Partially indistinct (25-50%)	Moderately indistinct (50%-75%)	Mostly indistinct (≥75%)
Tidemark	No visible	<25%	25-50%	50-75%	≥75%